



5th Multiphase Flow Journeys
May 17th-18th, 2019, Rio de Janeiro, RJ, Brazil

JEM-2019-0012

GAS-LIQUID FLOW PATTERN RECOGNITION USING DIMENSIONLESS NUMBERS

Caio César Silva Araujo
Tiago Ferreira Souza
Maurício de Melo Freire Figueiredo
Valdir Estevam
Ana Maria Frattini Fileti

University of Campinas, Av. Albert Einstein, 500, CEP 13083-852. Cidade Universitária, Campinas –SP, Brasil.

caio_cesar_unicamp@hotmail.com, tiagofs799@gmail.com, mauriciomff@gmail.com, valdir.est@gmail.com
frattini@feq.unicamp.br.

Abstract. Gas-Liquid two-phase flow is very frequent in process industries. The necessity to determine the flow pattern is mainly related to the need for design and monitoring the flow. To present a way to monitor the two-phase liquid-gas flow pattern, the sensitivity of the dimensionless number as a flow pattern classifier was performed. The dimensionless numbers evaluated were the Reynolds, Weber, Froude, Slippage Number and the pressure ratio. The configurations of flow studied were dispersed bubble, slug and churn flow patterns. To reach this objective, an experimental apparatus was built in the Experimental Laboratory of Petroleum (LabPetro) at the Center for Petroleum Studies (Cepetro), located at the University of Campinas (Unicamp). Experimental data was collected, using water or oil as a continuous phase and air as a dispersed phase. A high-speed camera was used to verify the actual flow pattern and compare with Taitel et al. (1980) flow map. The results indicate that Froude of the mixture and Weber Liquid numbers better recognize distinct regions of the flow patterns.

Keywords: Flow Pattern, dimensionless number, flow map, two-phase flow

1. INTRODUCTION

Multiphase flow is of great interest to the industry because it is usual to occur in industrial processes. One of the differences between single and two-phase flow is the existence of flow patterns. The term flow patterns refers to a set of specific geometric configurations in the flow delimited by interfaces. Process monitoring and analysis requires the determination of these different arrangements of the phases to infer about important design properties, such as void fraction and pressure gradient (Shoham, 2006). Thus, the monitoring system must be based on reliable and general parameters. In order to determine a parameter that covers broadly the flow, we present an analysis based on dimensionless numbers.

Chen (2006) suggests that, for capillary tubes, $1 < d < 5$ mm, Weber number best describes the flow and might be used to describe multiphase flow in small diameter pipelines. As the Weber number takes into account surface tension forces, it might be considered a strong candidate to describe the interface phenomenon, which is one of the main points in flow pattern analysis. Fukano and Kariyasaki (1993) suggested that, for large diameter (> 9 mm), the surface tension exhibit small influence than gravity and inertial forces, which indicates that Froude and Reynolds would be stronger candidates.

Abdelsalam *et al.* (2016) presented a new dimensionless number called Slippage Number (SL) which is based on the ratio of gravitational forces and inertia and takes into account the slippage between phases. The authors performed an extensive analysis of the relation between the SL and the Froude mixture number (Fr_m) and found an exponential relationship between them. No clear relation to the determination of flow pattern was obtained by the authors.

From the above, the objective of this work is to analyze the results obtained experimentally evaluating the sensitivity of the dimensionless numbers Reynolds, Weber, Froude, Slippage Number and pressure ratio. Afterward, determine the dimensionless numbers that can provide a clearer and more reliable information about the flow pattern in two-phase liquid-gas flows.

2. METHODOLOGY

To reach the objective of verifying the sensitivity of dimensionless numbers in flow pattern identification, the methodology was divided in two parts, being the first related to the experimental apparatus and the second to the dimensionless numbers.

2.1 Experimental Setup

A schematic view of the experimental apparatus constructed at LabPetro/Unicamp is presented in Figure 1. The test grid is divided into 3 lines: (i) Single phase for air, (ii) single phase for liquid and (iii) two-phase line which combined liquid and gas. The two phase line is a 52.5mm ID straight steel pipe of 10.4m long, beginning in the injector point, where the two-phase flow begins, and finishing in the liquid tank, where the two phases are separated. A volumetric pump controlled by a frequency inverter supply the liquid and a pressure vessel the air, that is controlled by a pressure regulator valve. The phase velocities were obtained using two flow meters, one for the gas and another for the liquid line, and the fluid properties obtained as function of the pressure and temperature. A high-speed camera was used to verify the flow pattern and compare with Taitel *et al.* (1980) flow map. Some points presented a mismatched between Taitel *et al.* (1980) flow map and visual classification. Thus, the analysis by dimensionless number was performed only for the points that both classifications agreed. The properties of viscosity and superficial tension were obtained by a rheological characterization. The annular flow pattern was not reached due to limitations in the test rig. The total of experimental points was 816, being 408 for water and 408 for oil. For each liquid, data were collected from 36 experimental points for dispersed bubble, 36 for slug and 30 for churn flow pattern with four repetition each experimental point.

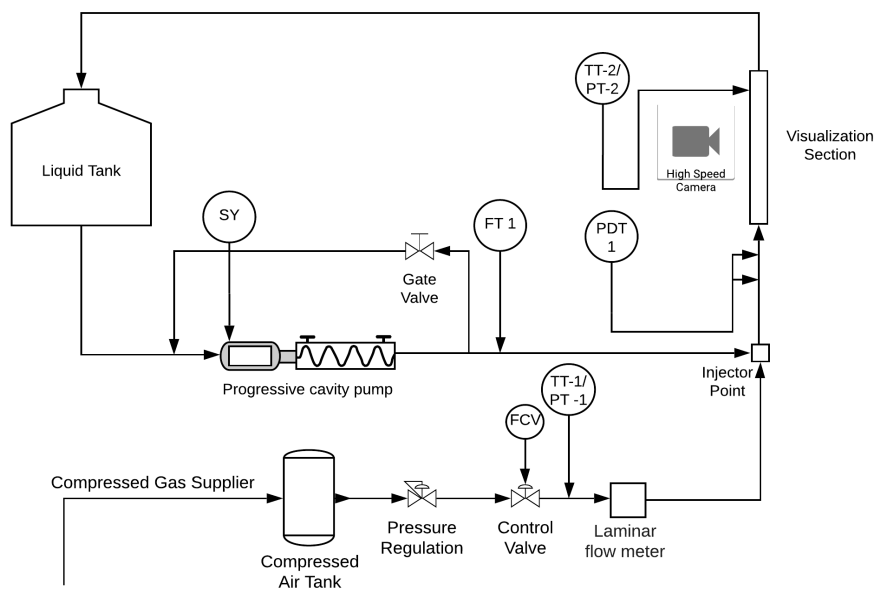


Figure 1. Schematic view of the Experimental Apparatus (LabPetro/Unicamp).

In the liquid line, a progressive cavity pump controlled by frequency inverter (SY), model NM053, from the manufacturer Netzsch, coupled to a WEG motor of 25 cv was used to pump the continuous phase. The oil line also had a Coriolis flowmeter (FT 1), model RHM40, provided by Metroval. In the air line was installed a pressure regulation valve, a pressure control valve (FCV), a laminar flow element containing a temperature transmitter (TT-1 and TT-2) and a pressure transmitter (PT-1 and PT-2), and a differential pressure transmitter (PDT-1). The gas control valve, model BR225, is of proportional control globe type with a motorized actuator, supplied by Holter Regelarmaturen. The laminar flow element, supplied by Merian, model 50MW20, has a calibration from 0 to 0.227 m³/min. In order to calculate the mass flow through the laminar element, the temperature of the flow was measured with a temperature transmitter supplied by the manufacturer Novus, model ED-Pt100, with the scale from 0 to 100 °C; pressure with the Rosemount Model 2051 Pressure Transmitter with calibration from 0 to 10 bar. Downstream of the injector nozzle, a temperature transmitter (TT-2) and a pressure transmitter (PT-2) were installed, with the same specifications as the air-line transmitters.

2.2 Dimensionless Numbers

The mathematical equations of the dimensionless numbers followed by a discussion about the balance of forces are presented here.

$$\text{Reynolds of Superficial Gas velocity } (Re_g) = \frac{\rho_g \cdot j_g \cdot d}{\mu_g} \quad (1)$$

$$\text{Reynolds of Superficial Liquid velocity } (Re_l) = \frac{\rho_l \cdot j_l \cdot d}{\mu_l} \quad (2)$$

$$\text{Reynolds Two-Phase } (Re_{tp}) = \frac{\rho_l \cdot (j_l + j_g) \cdot d}{\mu_l} \quad (3)$$

$$\text{Weber Two-Phase } (We_{tp}) = \frac{(j_l + j_g) \cdot \rho_l}{\mu_l} \cdot \frac{\sigma}{(\rho_l - \rho_g) \cdot g}^{1/2} \quad (4)$$

$$\text{Weber Liquid } (We_l) = \frac{\rho_l \cdot j_l^2 \cdot d}{\sigma} \quad (5)$$

$$\text{Pressure Ratio } (PR) = \frac{P}{P_{atm}} \quad (6)$$

$$\text{Slippage Number } (SL) = \frac{((H_l \rho_l + (1 - H_l) \rho_g) - \rho_h) \cdot g \cdot d}{\rho_g \cdot j_g^2} \quad (7)$$

$$\text{Froude of the mixture } (Fr_m) = \frac{\rho_l}{(\rho_l - \rho_g)}^{1/2} \cdot \frac{(j_l + j_g)}{(g \cdot d)^{1/2}} \quad (8)$$

Where, j_l and j_g are the superficial velocity of liquid and gas, ρ_l and ρ_g are the density of liquid and gas, μ_l and μ_g are the viscosity of liquid and gas, d is the pipe diameter, g is the gravity and σ is the surface tension, P is the pressure in the flow, P_{atm} is the atmospheric pressure, ρ_h is the homogeneous density and H_l is the in situ liquid holdup.

A variety of dimensionless numbers are present on literature relating main physicals parameters in multiphase flow, i.e. superficial velocity, density, viscosity, surface tensions, pipe diameter, and pressure as can be seen, e.g. at Ipsen (1960), Duns and Ros (1963), Dukler *et al.* (1964), Godbole *et al.* (2011), Nakashima (2015) and Figueiredo *et al.* (2016). The selected numbers were based on the main forces acting on dispersed, slug and churn flow patterns in vertical pipeline.

Each of these flow patterns has particular features. The dispersed bubble is governed by a balance between surface tension and turbulence forces (Shoham (2006)). In this way, the pattern remains dispersed bubble essentially when the turbulence is high enough compared to surface tension to keep a balance in coalescence and break of bubbles. In the slug flow either the transition from bubble to slug and slug to churn is mainly governed by an increase of the gas superficial velocity while the liquid superficial velocity is kept low. The bubble to slug transition occurs when the increase in the concentration of bubble is sufficient to coalesce and form the Taylor bubble. Sreenivas (2011) suggests that slug to churn transition occur when the Taylor bubble can flood the liquid that is falling around, as a result the Taylor bubble became unstable and deforms the surface. The churn flow is a complex flow-pattern, treated as a transition between slug and annular flow patterns, and the maximum velocity of liquid that does not occur (Sreenivas, 2011). A brief meaning of the numbers selected is presented next.

Reynolds number, Eq. (1) to Eq. (3), is a number that relates inertial and viscous forces. Interface phenomena are related to Weber number, Eq. (4) and Eq. (5), which represents liquid to capillarity forces ratio. Pressure ratio, Eq. (6), is a ratio between absolute measured and atmospheric pressure. Slippage number, Eq. (7), modify the Froude number in order to consider the slippage between the phases. Thus, it is defined as the difference in the gravitational forces between slip and no-slip conditions to the inertial force of the gas ratio. Finally, Froude number, Eq. (8), represents inertial to gravity forces ratio.

3. RESULTS AND DISCUSSION

The experimental results for the eight dimensionless groups used in this work are presented in Fig. 2 and Fig. 3. The results are expressed with homogeneous void fraction (GVF_h) axis to keep the dimensionless characteristic of the analysis and also because it is a well-known parameter in literature of multiphase flows. The data include the experimental results for water (black) or oil (red), as continuous phase, and air, as dispersed phase, in dispersed bubble, churn and slug flow patterns.

From Fig. 2 and Fig. 3 is possible to notice some dimensionless features with the present data. For both fluids, the dimensionless graphs present similar quantitative behavior, except for Re_l , Re_{tp} , and We_{tp} that present different results

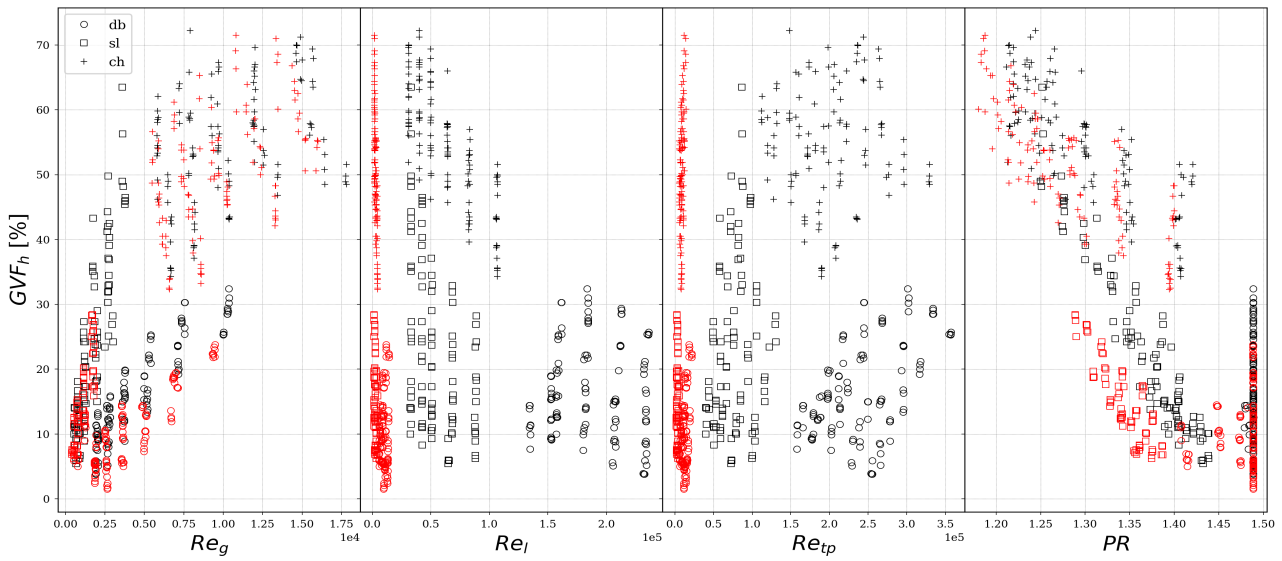


Figure 2. Reynolds and Pressure Ratio numbers versus homogeneous void fraction.

from oil to air. As can be noted, the We_l and Fr_m presented a clear delimiting region between dispersed bubble (db) and slug (sl) flow patterns. Re_g and PR do not demonstrate clearly frontier among the three patterns as a region or a single dimensionless number. Finally, the Fig. 3 suggested SL number as a slug classifier, once the data is mainly concentrated around 0 value except for slug flow pattern.

The results showed that the transition to the churn flow pattern is more dependent on homogeneous void fraction than the dimensionless number, suggesting a region above which the churn pattern is more likely to occur. The value 40 % of GVF_h is the best reference value to define the region above the churn flow pattern is more likely to occur. This value was defined based on a statistical analysis as follows (i) maximum percentage of churn to total data above the defined value (ii) minimum amount of churn to total data below the line and (iii) this value was define based on We_l and Fr_m .

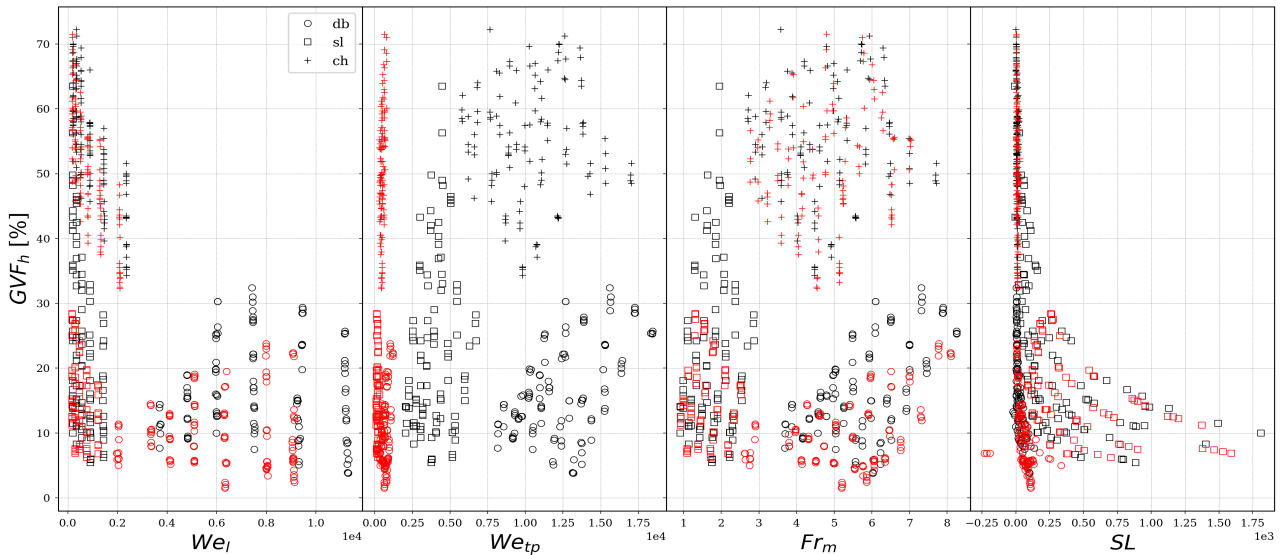


Figure 3. Weber, Froude and Slippage numbers versus homogeneous void fraction.

The Figure 4 is a representation in another x-scale for Re_l , Re_{tp} and We_{tp} . We can note that although in a qualitative way the results are similar, the quantitative behavior is different. This difference is almost constant for experimental points in an order of magnitude. Observing the equations related to these numbers we note that a liquid viscosity on the denominator is the source of difference. However, from the Figure 4, it became clear that these numbers are sensitive to flow pattern.

As can be seen in Fig. 5, is possible to distinguish between the flow patterns using just We_l and Fr_m , even for different continuous phases. For $Fr_m \leq 2,6$, the flow pattern will be slug. If $We_l \geq 3000$, the flow pattern will be dispersed bubble and it will be churn if $We_l \leq 3000$ and $Fr_m > 2,6$. The result that Fr_m and We_l may define flow pattern is also showed

in literature. Figueiredo *et al.* (2016) presented results of artificial neural network for flow pattern prediction based on PR , Re_l , We_l , We_{tp} , Fr_m numbers. Al-Sarkhi *et al.* (2017) proposed a new stratified to non stratified transition criterion horizontal flow based only on the Froude number. This transitions values was compared with a large database from the literature and a good agreement was obtained.

The Slippage number (SL) was illustrated in another scale (Figure 5). It is possible to observe that there are regions on graph that indicate sensitivity to flow pattern, however no clear limit related to the dimensionless number is defined. Although Abdelsalam *et al.* (2016) delimited regions on SL versus Fr_m graph suggesting a flow pattern classifier, no limits with respect to GVF_h versus SL was found. Thus, suggesting that this number is not proper to act as simple flow pattern classifier.

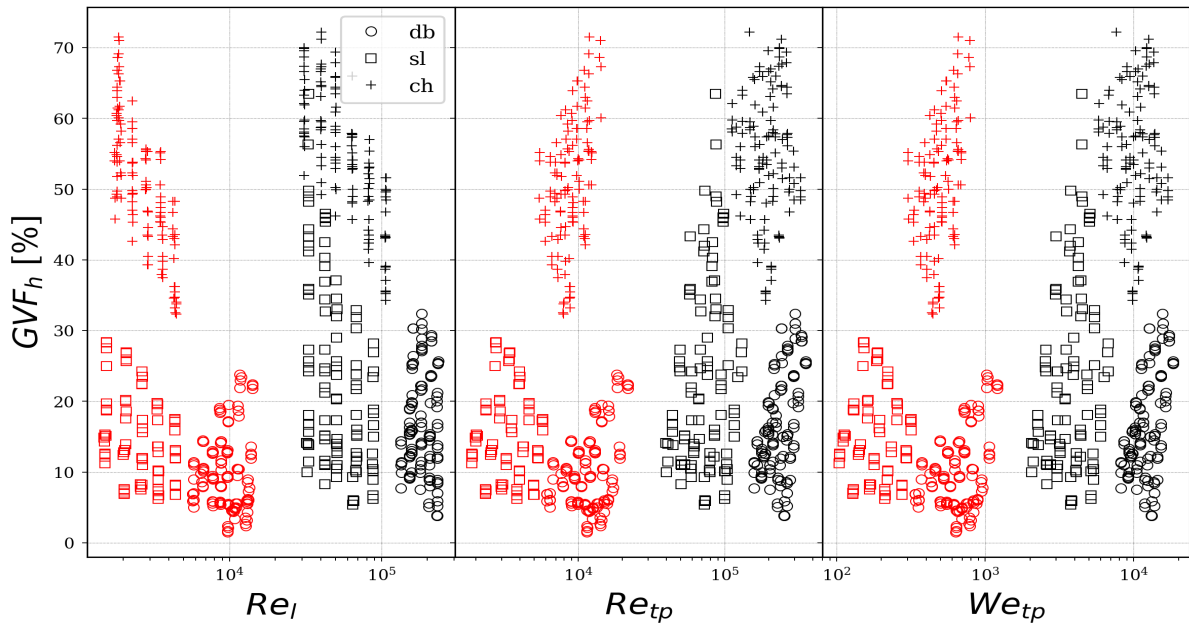


Figure 4. Re_l , Re_{tp} and We_{tp} present one order of magnitude difference for oil and water as a continuous phase.

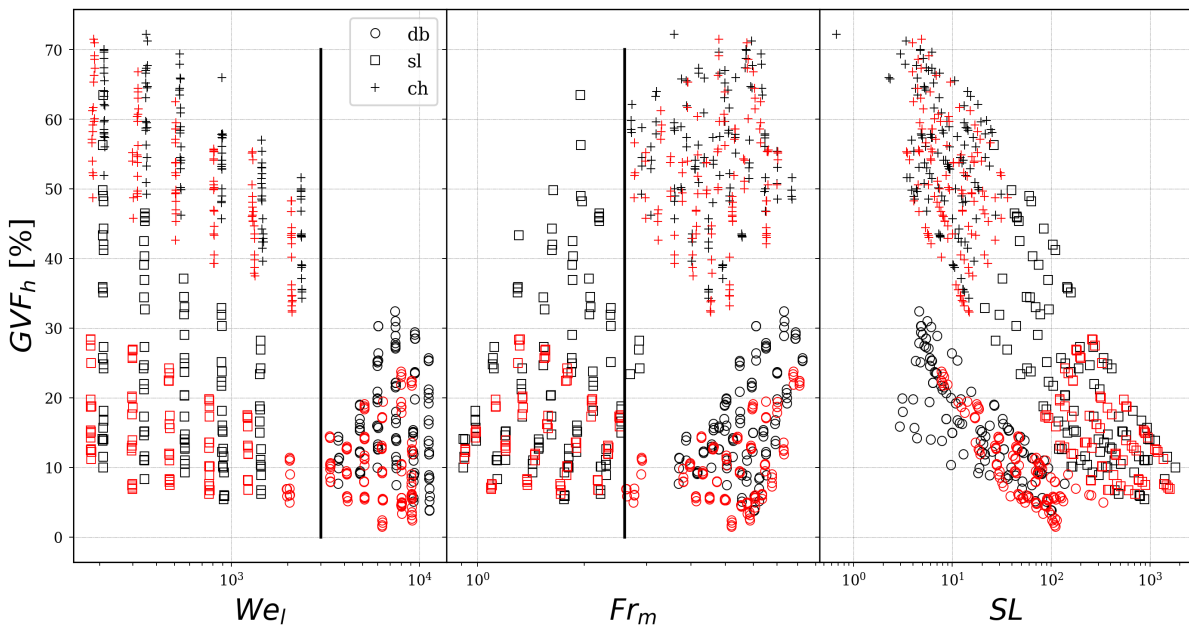


Figure 5. Froude of the mixture and Weber liquid as a flow pattern classifier. Slippage Number was not able to separate flow patterns.

4. CONCLUSIONS

This work presented an analysis based on the dimensionless number for two-phase flow to determine the sensitivity of Reynolds, Weber, Froude, Slippage Number and pressure ratio as a flow pattern classifier, using water or oil as the continuous phase and air as the dispersed phase.

The main conclusion arising from this work is that We_l and Fr_m could successfully classify slug, churn and dispersed bubble flow patterns. The results showed that the flow pattern churn is more dependent to GVF_h than any of the dimensionless numbers presented.

5. ACKNOWLEDGEMENTS

The authors are thankful for the support of Petrobras/ANP. The authors also acknowledge the Center For Petroleum Studies (CEPETRO - Unicamp), CNPq and CAPES.

6. REFERENCES

- Abdelsalam, A., Cem, S. and Eduardo, P., 2016. "New dimensionless number for gas-liquid flow in pipes". *International Journal of Multiphase Flow*, Vol. 81, pp. 15–19. ISSN 03019322. doi:10.1016/j.ijmultiphaseflow.2015.12.008. URL <http://dx.doi.org/10.1016/j.ijmultiphaseflow.2015.12.008>.
- Al-Sarkhi, A., Pereya, E., Mantilla, I. and Avila, C., 2017. "Dimensionless oil-water stratified to non-stratified flow pattern transition". *Journal of Petroleum Science and Engineering*, pp. 287–291. doi: <https://doi.org/10.1016/j.petrol.2017.01.016>.
- Chen, L., 2006. "Flow Patterns in Upward Two-Phase Flow in Small Diameter Tubes".
- Dukler, A.E., Wicks, M. and Cleveland, R.G., 1964. "Frictional pressure drop in two-phase flow: B. An approach through similarity analysis". *AICHE Journal*, Vol. 10, No. 1. doi:<https://doi.org/10.1002/aic.690100118>.
- Duns, H. and Ros, N., 1963. "Vertical Flow of Gas and Liquid Mixtures in Wells."
- Figueiredo, M.M.F., Gutierrez, J.E.L., Pineda Perez, H.A., Fileti, A.M.F., Ratkovich, N.R. and Carvalho, R.D.M., 2016. "The use of Artificial Neural Networks for flow pattern identification and GVF determination in two-phase flows". In *Modelling, Simulation and Identification*. Campinas. doi:10.2316/P.2016.841-011.
- Fukano, T. and Kariyasaki, A., 1993. "Characteristics of gas-liquid two-phase flow in a capillary tube". *Nuclear engineering design*, pp. 59–68.
- Godbole, P.V., Tang, C.C. and Ghajar, A.J., 2011. "Comparison of Void Fraction Correlations for Different Flow Patterns in Upward Vertical Two-Phase Flow". *Heat Transfer Engineering*, Vol. 32, No. 10, pp. 843–860. doi: 10.1080/01457632.2011.548285.
- Ipsen, D.C., 1960. *Units, Dimensions, And Dimensionless Numbers*. McGraw-Hill.
- Nakashima, A.M.V., 2015. "Desenvolvimento de rede neurais utilizando técnica ultrassônica e números adimensionais para a determinação da fração de vazio e padrões de escoamentos multifásicos representativos na indústria do petróleo". *Msc*, p. 131.
- Shoham, O., 2006. *Mechanistic Modeling of Gas-Liquid Two-Phase Flow in Pipes*. ISBN 155563107X.
- Sreenivas, J., 2011. "Churn Flow". *Thermopedia*.
- Taitel, Y., Bornea, D. and Dukler, A.E., 1980. "Modelling Flow Pattern Transition for Steady Upward Gas-Liquid Flow in Vertical Tubes". *AICHE Journal*, Vol. 26, No. 3, pp. 345–354.

7. RESPONSIBILITY NOTICE

The authors are the only responsible for the printed material included in this paper.